Effective refractive index of drying droplet of water fullerene suspension

D. Jakubczyk, G. Derkachov, W. Bazhan, E. Łusakowska, K. Kolwas and M. Kolwas

Institute of Physics, Polish Academy of Sciences, al. Lotników 32/46, 02-668 Warsaw, Poland

ABSTRACT

Laser light scattering by a drying droplet of water fullerene suspension several micrometers in size was studied. Two light wavelengths were used. The evolution of refractive index and radius of the droplet was investigated. Resonant scattering was identified and analyzed. Some conclusions were drawn on the microscopic properties of the suspension. Supplementing measurements of samples obtained by drying the water fullerene suspension and toluene solution were conducted with Atomic Force Microscope (AFM).

Keywords: effective refractive index, fullerene suspension, C_{60}, resonant scattering

1. EXPERIMENT

We adopted a static light scattering technique for the investigation of the atmospheric aerosols. This technique enables to follow the evolution of the radius of the droplet $R(t)$ of the evaporating suspension and of its effective refractive index $\varepsilon_{eff}(R)$. We observed that evaporating droplets of suspension exhibit discrepancy of their refractive index as a function of inclusions density from standard effective medium theory prediction. We developed a simple model of scattering of light by a single droplet of water containing fullerene (C_{60}) nanocrystallites.[1] By these means we tried to infer about the physical properties of the suspension. We supplemented our investigation with an AFM study of samples obtained by drying the suspension and toluene solution.

The diagram of experimental setup is presented in figure 1. The detailed description of our experimental setup

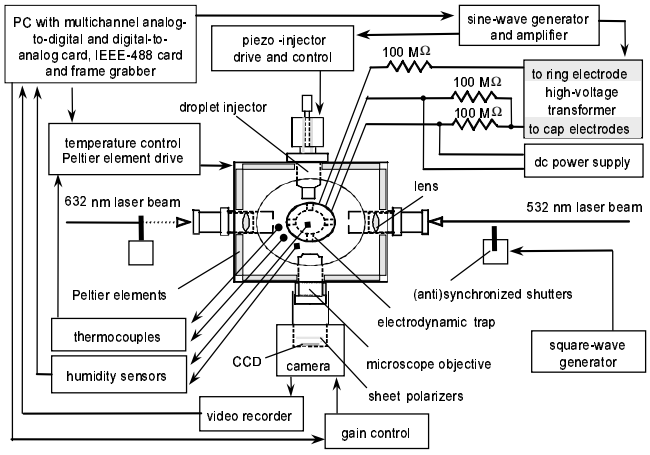

Figure 1. Experimental setup.

and procedures can be found in.[1,2] C_{60} nanocrystallites water suspension was prepared by stirring or sonicating C_{60} powder in distilled water and filtering shortly before the experiment. At the stage of preparation we were not able to estimate the concentration of suspension. The thermodynamic conditions of our experiments are given in figure 3 caption. The AFM was operated in the tapping mode and the tip curvature radius was ~ 20 nm.

Send correspondence to: Daniel Jakubczyk, E-mail: jakub@ifpan.edu.pl

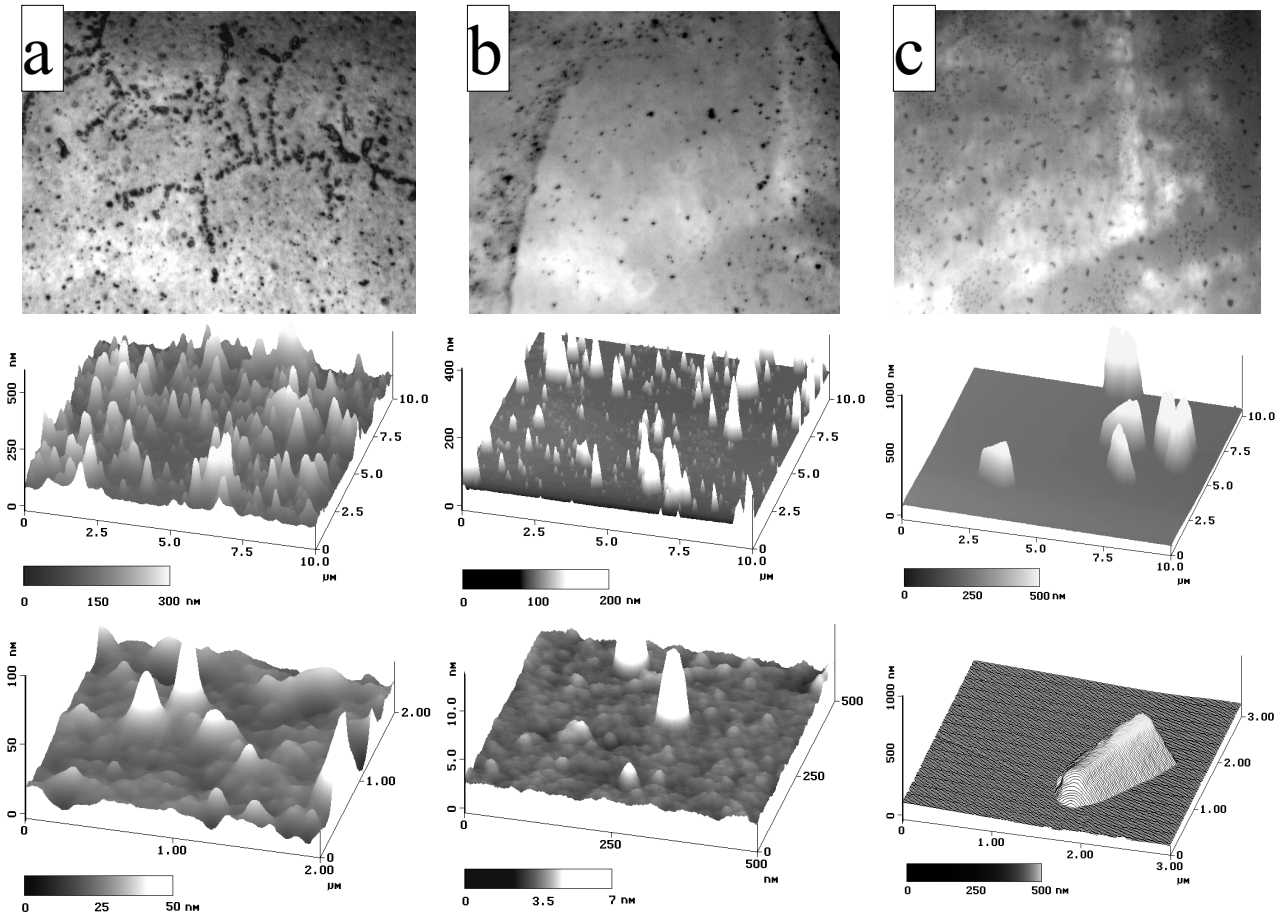

Figure 2. Top, optical microscopy, $\sim 500\times$ magnification; bottom, AFM images, 3D representation, two magnifications, of a sample obtained by: (a) air drying and (b) spin coating of the water C_{60} suspension and (c) spin coating of C_{60} toluene solution.

We used two types of samples for the AFM measurement. A drop of about 3 μl of C_{60} suspension was: (i) air-dried or (ii) spin-coated on the cover glass. In case of the air dried sample, all the C_{60} material remained on the glass. Then we were able to find the average C_{60} layer thickness with AFM measurement and estimate the initial C_{60} mass concentration to be ~ 3 μg/ml. Aggregates of average radius from ~ 8 nm to ~ 500 nm (figure 2a) were found in these samples. The aggregates size distribution was of a power-law type. This indicated[3] that the aggregation must have been diffusion limited and had lead to fractal clusters. In the spin-coated sample a fine crystallite fraction dominated (figure 2b). Mechanical method of suspension preparation seems to favor coarse and very fine fraction. Coarse fraction gets filtered out. Since most of the suspension drop leaves the cover glass while spin-coating, there is also no time for secondary aggregation into a coarse fraction. The comparison of figures 2a and b indicates that it is aggregation, due to water evaporation, from fine crystallites, that is responsible for microscopic properties of suspension droplet at the later stages of the droplet evolution. We estimated the diameter of the elementary building block to be ~ 8 nm. For comparison, we present the image of crystallites grown in ambient air from saturated toluene solution after spin-coating (figure 2c). The size distribution was dramatically narrower. In figure 3 we present two quite different $\varepsilon_{eff}(R)$ evolution scenarios corresponding to $R(t)$ evolutions. Figures 3a correspond to a particle with high C_{60} content, nearly dry in the end, while figures 3b correspond to a particle of rather low C_{60} content. The Mie scattering patterns persisted all the time, not giving way to "bulk speckle". This could be caused by high deliquescence of particle as well as by absence of structures large enough. Since our AFM observations as well as revealed a wide spectrum of C_{60}

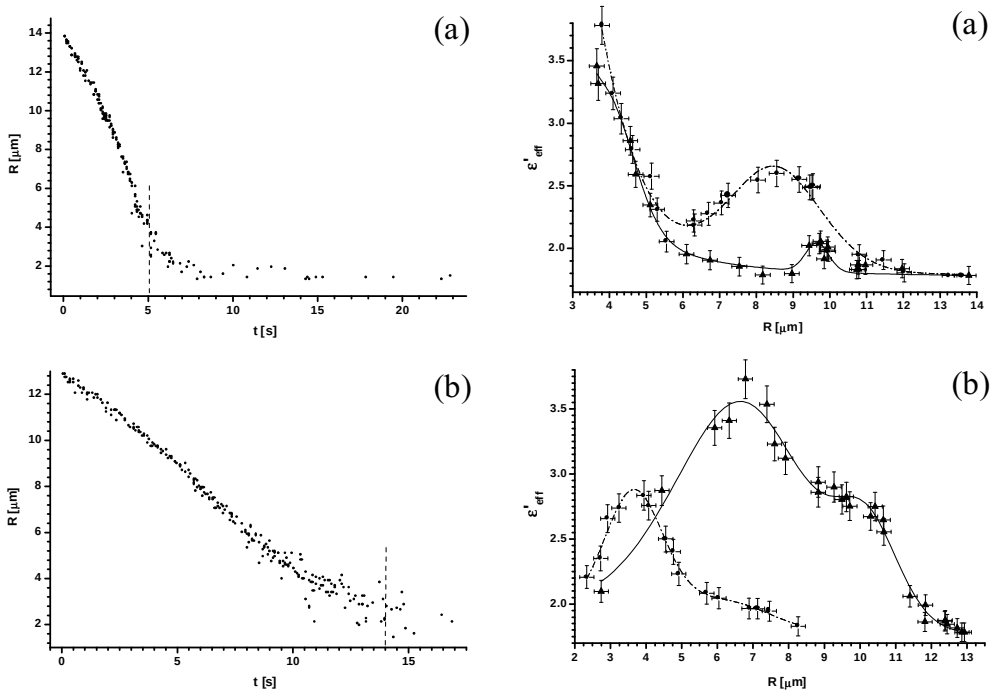

Figure 3. Left, evolution of the composite droplet radius for: (a) high fullerene contents, temperature $T = 294.9$ K, relative humidity $S = 95$ %, atmospheric pressure $p_{atm} = 979$ hPa and (b) low fullerene contents, $T = 296.3$ K, $S = 98$ %, $p_{atm} = 1006$ hPa. Right, the real part of effective dielectric function of the composite droplet as a function of droplet radius, corresponding to figures on the left; circles and dash-dot line - green light and triangles and solid line - red light.

nanocrystallite sizes in suspension, we would expect very few voids in the totally dry polycrystalline particle. For C_{60} nanocrystallites suspension we might expect small but non-negligible imaginary part of refractive index, when the packing becomes dense. However, the effect was hardly perceivable. This would indicate that the particles may stabilize as wet. In this paper we dealt only with wet particles with purely real refractive index (left of the vertical dashed lines in figure 3). For the suspension of C_{60} nanocrystallites in water the aggregation and percolation of solid phase can take place and the inclusions may be highly polydyspersive. Thus we could encounter two kinds of resonances: (i) associated with C_{60} structures size and (ii) associated with the average distance between neighboring C_{60} structures. As the droplet shrinks due to the evaporation, the size of C_{60} structures grows, while the distance between them diminishes. Since the light scattering experiment was conducted for two wavelengths simultaneously, we were able to distinguish the type of resonance by its relative position for green and red light versus the droplet radius. In both figures the resonance for red light is shifted to the right in comparison to the same for green. Thus we infered that we encountered resonances of type (ii). This would indicate that the aggregates usually do not grow to the size enabling resonant behavior, which we would expect near half the light wavelength $\lambda/2$.

2. DISCUSSION

In order to further interpret our experimental results, we adopted the Maxwell-Garnet mixing rule, which holds for very low and very high filling factors, and corrected it in a phenomenological way for mid-range filling factors.[1] For inclusions of dielectric function ε_f, essentially smaller than λ, uniformly distributed in a medium the total polarizability can be expressed after Wiener as:

$$\sum_j n_j \alpha_j = f \frac{\varepsilon_f - \varepsilon_m}{\varepsilon_f + 2\varepsilon_m} \cdot 3\ \varepsilon_0 \varepsilon_m \tag{1}$$

where n_j and α_j are the number density and polarizability of the j-th particle species, ε_m is the dielectric function of the medium and $f = (3V_{dry})/(4\pi R^3)$ is filing factor. A composite medium can be perceived as composed of a set of harmonic oscillators. Under ordinary conditions there exists a nonuniform distribution of characteristic frequencies ω_k, arising from e.g. nonuniform spatial distribution of density of different species n_j. This leads to a gaussian profile of resonance. This broadening Modifying the density of the composite medium should lead to manifestation of various resonances. We describe the total polarizability by the series of resonators, with naturally distributed resonance frequencies. Since the expression should hold for the limiting cases - a very small and a very large filling factor - we write:

$$\sum_j n_j \alpha_j = \frac{1}{R^3}\left\{ A_0 + \sum_{k>1} A_k \exp\left[-\left(\frac{\omega - \omega_k}{\gamma_k} \right)^2 \right] \right\} \ , \ A_0 = V_{dry} \frac{\varepsilon_f - \varepsilon_m}{\varepsilon_f + 2\varepsilon_m} \ , \tag{2}$$

where $\omega = 2\pi c/\lambda$, γ_k describes resonance width and A_k is a constant. The frequencies ω_k should correspond to characteristic sizes r_k of structures involved: $\omega_k \sim 1/r_k$. For resonances associated with average distance between neighboring inclusions, r_k should, in turn, be proportional to R: $\omega_k = C_k/R$, where C_k is a constant. Then $(\omega - \omega_k)/(\gamma_k) = (\omega - C_k/R)/(\gamma_k)$. Finally, we can rewrite the Maxwell-Garnet mixing rule as follows:

$$\varepsilon_{eff} = \varepsilon_m \frac{1 + (2M(R))/(R^3)}{1 - (M(R))/(R^3)} \ , \text{ where } M(R) = A_0 + \sum_{k>1} A_k \exp\left[-\left(\frac{\omega - C_k/R}{\gamma_k} \right)^2 \right] \ . \tag{3}$$

The factor M can be perceived as a modification of the local field arising from multipolar effects of scattering on inclusions,[4] near field effects,[5] interference of fields multiply scattered along different paths,[6] etc. The experimental data presented in figure 3 was fitted with formula 3. We used the smallest reasonable value of k. One and two resonances were imitated for data presented in figures 3a and b respectively. Then we tried to infer about the size of C_{60} nanocrystallites involved. The aggregation scenario is assumed to be diffusion limited.[3] On the basis of our AFM study we can assume that at the middle stage of the evolution when the resonance is observed, there is a distribution of inclusion sizes in which finer fractions prevail. In case of the evolution leading to the dry or nearly dry particle, as in figure 3a, $R(t \to \infty)$, is known. We further assume that inclusions associated with the resonance make up $0.75V_{dry}$ and that the average distance between neighboring scatterers associated with the resonance is of the order of λ/n_w, where n_w is the real part of the refractive index of water. Then, the approximate average radius of the scatterer in question $r_{incl} \simeq R(t \to \infty)(\lambda)/(2R_{res}n_w)$, where R_{res} is the radius of the composite droplet corresponding to the resonance. For the evolution presented in figures 3a, $R(t \to \infty) = 1.41$ μm, $R_{res}(red) = 9.64$ μm and $R_{res}(green) = 8.47$ μm, and $n_w(red) = 1.33209$ and $n_w(green) = 1.33551$. We obtained $r_{incl}(red) \simeq 35$ nm and $r_{incl}(green) \simeq 33$ nm which is in agreement with the AFM observations (figures 2a and b). Thus we can conclude that $r_{incl} \simeq 34$ nm.

ACKNOWLEDGMENTS

This work was supported by Polish State Committee for Scientific Research grant 2 P03B 102 22.

REFERENCES

1. D. Jakubczyk, G. Derkachov, M. Zientara, M. Kolwas and K. Kolwas, "Local-field resonance in light scattering by a single water droplet with spherical dielectric inclusions," *J. Opt. Soc. Am. A* **21**, 2004 in print.
2. D. Jakubczyk, M. Zientara, W. Bazhan, M. Kolwas and K. Kolwas, "A device for light scatterometry on single levitated droplets," *Opto-Electron. Rev.* **9**, 423-30, 2001.
3. G. V. Andrievsky, V. K. Klochkov, E. L. Karyakina and N. O. Mchedlov-Petrossyan, "Studies of aqueous colloidal solutions of fullerene C_{60} by electron microscopy," *Chem. Phys. Lett.* **300**, 392–6, 1999.
4. P. Chýlek, V. Ramaswamy and R. J. Cheng, "Effect of graphitic carbon on the albedo of clouds," *J. Atmos. Sci.* **41**, 3076–84 1984.
5. H. Xu, "A new method by extending Mie theory to calculate local field in outside/inside of aggregates of arbitrary spheres," *Phys. Lett. A* **312**, 411–9, 2003.
6. B. A. van Tiggelen, A. Lagendijk, M. P. van Albada and A. Tip, "Speed of light in random media," *Phys. Rev. B* **45**, 12233–43, 1992.